Interfacial Roughening Induced by the Reaction of End-Functionalized Polymers at a PS/P2VP Interface: Quantitative Analysis by DSIMS

Bumjoon J. Kim,[†] Huiman Kang,[‡] Kookheon Char,[‡] Kirill Katsov,[†] Glenn H. Fredrickson,[†] and Edward J. Kramer*,[†]

Department of Materials and Chemical Engineering, University of California, Santa Barbara, California 93106, and School of Chemical Engineering and Institute of Chemical Processes, Seoul National University, Seoul 151-744, Korea

Received December 20, 2004; Revised Manuscript Received February 22, 2005

ABSTRACT: The reaction of end-functionalized polymer chains at the melt interface between the immiscible polymers, polystyrene (PS) and poly(2-vinylpyridine) (P2VP), has been investigated experimentally. Diblock copolymers were formed at the interface by the reaction of amine end-functionalized deuterated PS with anhydride end-functionalized P2VP. The normalized interfacial excess ($\xi = z^*_{PS}/R_{g,PS}$) of the deuterium-labeled block copolymer was determined using dynamic secondary ion mass spectrometry (DSIMS). As ξ increases, the interfacial tension decreases to zero, at which point the interface becomes unstable, inducing interfacial roughening by hydrodynamic flow of the homopolymers. Roughening was detected using scanning force microscopy (SFM) after removing the polystyrene with a selective solvent. Evidence of the interfacial instability was also observed by cross-sectional transmission electron microscopy (TEM). The length scale of the corrugation was around 15 nm, which was comparable to the diameter of diblock copolymer emulsified droplets found near the interface. For a short symmetric block copolymer (PS (4K)−P2VP (4K)), we observed that the interfacial roughening takes place above $\xi = 0.9$, in good agreement with the predictions of self-consistent mean-field theory.

Introduction

The interface between strongly immiscible polymer pairs is very sharp, and only a small extent of interpenetration of molecules is allowed due to the highly unfavorable enthalpic interaction between the chemically different polymers. The properties of sharp interfaces can be modified by the segregation of block copolymers,[1−7] which occurs due to the fact that the unfavorable interaction can be reduced by confining the block copolymer joints at the interface. However, an entropic penalty has to be overcome due both to block copolymer joint localization and to the stretching of the polymer blocks as the areal density of block copolymer increases.[8] Such segregation of copolymers to an interface leads to a decrease in the interfacial tension. The block copolymers are also very effective in suppressing coalescence of droplets of the dispersed polymer phase, even at very low areal chain densities.[9−12] One of the most effective methods to generate block copolymers at an interface is reactive blending of polymers containing two different types of end-functionalized polymers. The localization of diblock copolymers at the interface can be achieved in-situ by the reaction between the end-functionalized polymers. If the reaction produces enough block copolymer, an interfacial instability ensues, leading to the formation of small droplets, wherein the diblock copolymers form ordered or disordered mesostructures, similar to microemulsions. Such microemulsion phenomena have been widely investigated for various systems, for example, mixtures of oil, water, and surfactants.[13] Previous work on polymer blend systems has shown that microemulsions occur above a certain interfacial areal density of diblock copolymers. To minimize the amount of block copolymer (and thus the cost), it is important to determine the optimum amount of diblock copolymer and to understand the interfacial roughening and droplet formation phenomena better.

Roughening of immiscible polymer interfaces due to block or graft copolymer additives was visualized previously by several researchers,[14−21] and the decrease of interfacial tension was calculated approximately based on self-consistent mean-field theory (SCMFT) methods described by Shull.[22] Lyu et al.[17] investigated the interfacial roughening caused by the reaction of end-functionalized PS and PMMA at the interface between melts of the pure end-functional chains; i.e., there were no unfunctionalized homopolymer, PS or PMMA, present. They argued that thermal fluctuations cause the deformation of the diblock copolymer layer formed at the interface, leading to an increased interfacial area that allows further reaction of end-functionalized polymers, thus inducing the interfacial instability. They asserted that although the reduction of interfacial tension by diblock copolymers is a potential cause for interfacial roughening, the large interfacial roughening that they observed could be achieved without the interfacial tension vanishing. Since their experiment was done in a bulk system, they could not measure directly the areal chain density of diblock copolymers at the interface. Since measurements of the areal chain density are necessary to predict the change in interfacial tension, it is not clear what value of interfacial tension was achieved at the onset of the interfacial roughening in their system. On the other hand, Jiao et al.[15,16] estimated that the interfacial instability is due to the vanishing interfacial tension in a different system by comparing the onset point of interfacial roughness observed experimentally to the results of SCMFT. An

[†] University of California, Santa Barbara.
[‡] Seoul National University.
* To whom correspondence should be addressed. E-mail: edkramer@mrl.ucsb.edu.

10.1021/ma047378s CCC: $30.25
Published on Web 06/11/2005

amine-terminated deuterated polystyrene and a poly(styrene-*r*-maleic anhydride) (PSMA) random copolymer were used for the grafting in their system. However, since PSMA chains have many reactive anhydride groups at arbitrary positions along them, the application of SCMFT is significantly complicated, and the technique was not employed. In this case, the measured areal density of end-functionalized deuterated polystyrene could not be used to calculate the areal density of the other polymer, a grafted PSMA random copolymer. In their estimate they assumed that the only entropic penalty due to chain stretching was from the dPS brush. Any chain stretching of the PSMA was ignored. In addition, the Flory−Huggins interaction parameter χ between PS and PSMA was known only within very broad limits.

An ideal experiment to compare with predictions from SCMFT therefore remains to be carried out. The conditions for such an experiment are as follows: First of all, the reactive random block copolymers should be replaced by end-functionalized polymers that have only one functional group at the end, as in the experiment of Lyu et al.,[17] so that diblock copolymer chains of precise architecture are produced by the reaction at the interface. The important parameters of the system such as χ, diffusion coefficients, reaction chemistry, and so forth should be known. Particularly, the knowledge of χ enables SCMFT to predict accurately the interfacial tension of the system for a prescribed amount of diblock copolymers formed by the reaction at the interface. In addition, accurate information about chain areal density of diblock copolymers at the interface is crucial for the estimate of interfacial tension by SCMFT. Therefore, much effort has been made to measure the interfacial excess of diblock copolymers. These diblock copolymers need to be labeled, with either fluorescent groups or isotopes such as deuterium. The labeling technique allows one to measure the chain areal density of diblock copolymers formed by the reaction of end-functionalized polymers as well as to follow concentration gradients necessary for the study on the diffusion of labeled end-functionalized polymers to the interface. Jiao et al.[15,16] and Schulze et al.[23] synthesized the deuterated end-functional polymers and monitored the progress of the interfacial reaction using forward recoil spectrometry (FRES), which is a depth profiling technique. In addition, Schulze et al.[24] used anthracene-labeled end-functional polymers to measure the chain areal density of diblock copolymers formed by the interfacial reaction using size exclusion chromatography (SEC) with a fluorescence detector. They compared the interfacial excess of diblock copolymers from the reaction measured using FRES with that from SEC. They concluded that their interfacial coverage might be larger than that required for the onset of interfacial roughening. Jones and co-workers[19] also used end-functionalized polymers with anthracene-labeled groups to monitor the reaction of end-functionalized polymers at the interface, thus giving the chain areal density of diblock copolymers at the interface. They studied the effect of monomer structure on the reactions at the interface of immiscible polymers and found that the change in monomer structure of end-functional polymers produces a difference in diblock copolymer chain areal density formed by reaction at a given reaction time and observed the interfacial roughening in the system where different pairs of end-functionalized polymers were used. However, they did not analyze the mechanism for interfacial roughening quantitatively by calculating the interfacial tension at a given areal chain density.

We decided to use the end-functionalized polymers, deuterated polystyrene (dPS) with an amine end group and poly(2-vinylpyridine) (P2VP) with an anhydride end group, as a model reactive system. Our aim is to reveal the mechanism of interfacial roughening by comparing the experimental results with the theoretical predictions of SCMFT. The use of PS and P2VP is advantageous for several reasons. PS is highly immiscible with P2VP at all temperatures above the glass transition temperatures of PS and P2VP, which are quite similar (∼100 °C). In addition, the diffusion coefficients of PS and P2VP are believed to be similar for comparable molecular weight in both magnitude and temperature dependence.[25] All these similar properties help us investigate diffusion as well as reaction of the end-functionalized polymers in our system. Most importantly, the temperature dependence of χ between PS/P2VP has been determined.[26] In addition, there is considerable information on the reaction between polymers with anhydride and amine end-functional groups in the literature.[27−29] The reaction shown in Figure 1 yields a diblock copolymer at the interface.

We use dynamic secondary ion mass spectrometry (DSIMS), a well-established depth-profiling technique, to monitor the reaction and diffusion of the deuterium-labeled amine end-functionalized PS (dPS-NH_2). DSIMS has much better depth resolution (∼8 nm) than FRES (∼90 nm)[24] combined with high sensitivity and the ability to provide the profiles of all elements at the same time. All experiments were designed so that the block copolymers were formed at the interface in the dry brush regime.[8,30] This simplifies the SCMFT prediction of the interfacial tension for a given amount of diblock copolymer formed at the interface. Dry brush conditions were achieved by using a mixture of homopolymers with very high molecular weight and end-functionalized polymers with relatively small molecular weight. The combination of these experimental conditions and techniques makes our system much closer to an ideal model experiment for comparison with the SCMFT calculations than any of the previous experiments. While the short block copolymers that form can be expected to produce only minimal reinforcement of the interfaces in this PS/P2VP system, the results can be generalized to the reaction of longer end-functionalized polymer chains.

In this paper, we first study the reaction of end-functionalized polymers by quantifying the amount of diblock copolymers at the PS/P2VP interface using DSIMS. On the basis of the DSIMS characterization, the interfacial tension of the system is calculated using SCMFT and the Gibbs adsorption isotherm. The interfacial roughness of those samples was measured by scanning force microscopy (SFM) and also visualized by cross-sectional transmission electron microscopy (TEM). Finally, the onset for interfacial roughening is obtained in terms of the interfacial tension at a given concentration of diblock copolymers at the PS/P2VP interface. The comparison of the onset of interfacial roughening observed experimentally with the threshold for the vanishing of interfacial tension from SCMFT is expected to clarify the role of interfacial tension on the interfacial roughening and ultimately reveal a mechanism for interfacial roughening.

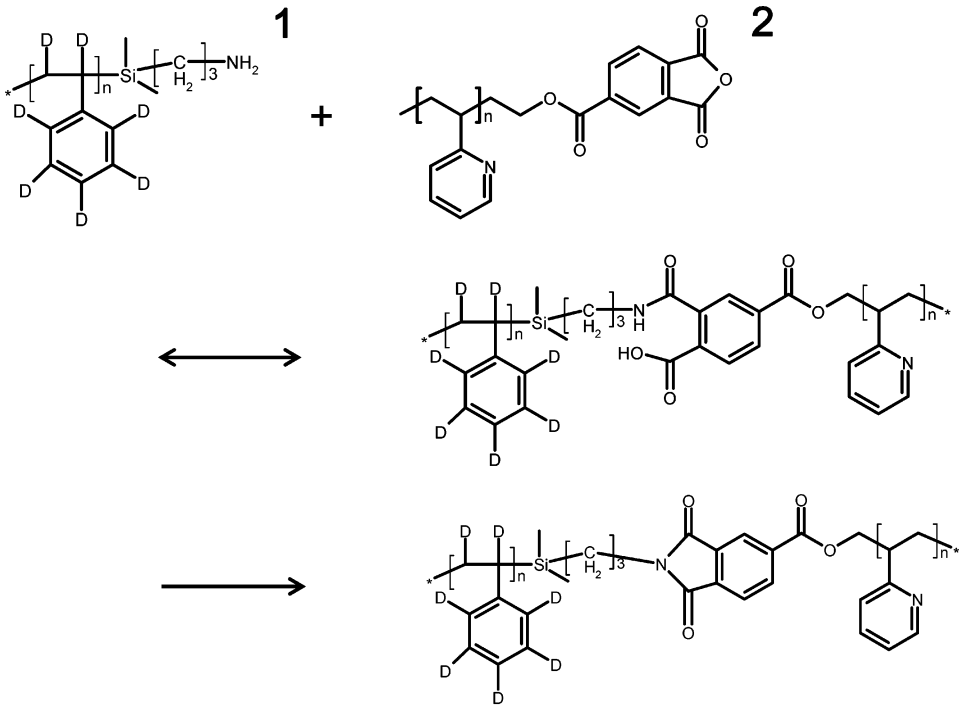

Figure 1. Reaction chemistry at the interface. Deuterated polystyrene with an amine end group reacts with poly(2-vinylpyridine) with an anhydride end group to form dPS−P2VP diblock copolymer.

Table 1. Characteristics of Polymers Used in the Present Study

polymer	M_n (kg/mol)	M_w/M_n	functionality
PS	207	1.06	0
P2VP	152	1.12	0
dPS-NH_2	4.3	1.05	0.7[a]
P2VP-ah	4.2	1.05	0.5[b]

[a] Measured by titration. [b] Obtained by coupling with PEG-NH_2 (M_n = 5K) and measuring the ratio of coupled product to unreacted polymers using SEC.

Experimental Section

Polymer Synthesis and Characterization. An amine end-functionalized deuterated polystyrene (dPS-NH_2), shown as **1** in Figure 1, was purchased from Polymer Source Inc. A PS homopolymer was kindly donated by Dow Chemical Inc. An anhydride end-functionalized poly(2-vinylpyridine) (P2VP-ah), **2** in Figure 1, was prepared by anionic polymerization. 2-Vinylpyridine (2-VP) monomers were dried over calcium hydride overnight and then over triethylaluminum for 3 h. Tetrahydrofuran (THF) was dried over *sec*-BuLi and degassed by three freeze−thaw cycles in a vacuum line. Next, THF was distilled into the reaction vessel. 2-VP monomer was added to the THF, and the polymerization was initiated by the addition of a calculated amount of *sec*-BuLi at −78 °C. After completion of the polymerization (3 h), the living anions were terminated with ethylene oxide[31] at −78 °C. An excess amount of trimellitic anhydride chloride was then added to the solution after the temperature was raised to 0 °C, and further reaction was carried out overnight. The resulting polymer was purified by precipitation in *n*-hexane. A PVP homopolymer was also synthesized by anionic polymerization and was terminated by degassed 1-butanol.

The characteristics of the polymers used in present study are summarized in Table 1. The molecular weight and polydispersity of the polymers were determined by matrix-assisted laser desorption/ionization mass spectrometry (MALDI) as well as by size exclusion chromatography (SEC) using PS standards. The specimens for the MALDI measurements were prepared by following the method described by Lim et al.[32] P2VP-ah or dPS-NH_2 was dissolved in dichloromethane at a concentration of 2×10^{-3} M. A solution of a matrix, dithranol, of 0.15 M in dichloromethane as well as a saturated solution of NaCl in ethanol was prepared. Initially, the matrix solution, the NaCl in ethanol solution, and polymer solution were mixed together in a volume ratio of 1:1:1. When the signal intensity was below the measuring sensitivity, the solution was prepared in a volume ratio of 2:1:1 in order to increase the signal intensity. The functionality of dPS-NH_2 was determined by a titration method and by ^{1}H NMR. The dPS-NH_2 polymer was titrated with $HClO_4$ to a violet end point in a 1:1 v/v solution of chloroform and glacial acetic acid using crystal violet as an indicator. The functionality obtained was double-checked by comparing the signals from the aliphatic protons next to the terminal amine group to the proton signals from the *sec*-butyllithium initiator in ^{1}H NMR. The functionality of P2VP-ah was obtained by SEC after reaction with PEG-NH_2 (M_n = 5 kg/mol) at 65 °C in THF for 8 h.

Sample Preparation for DSIMS. A 300 nm thick SiO_2 layer was deposited on a Si wafer by plasma-enhanced chemical vapor deposition (PECVD). All samples were prepared by spin-casting a 350−400 nm thick layer of a mixture of P2VP homopolymer with a number-average molecular weight (M_n) of 150 kg/mol and P2VP-ah with M_n = 4.2 kg/mol from a solution in anhydrous pyridine. The volume ratio of P2VP-ah to P2VP homopolymers was 0.12. A 450−500 nm thick layer of PS was then prepared on the top of the P2VP layer by spin-casting a mixture of 207 kg/mol PS homopolymer and 4.3 kg/mol dPS-NH_2 from toluene solution. The volume ratio of dPS-NH_2 to PS homopolymer in PS layer was also fixed at 0.12. The samples were annealed at temperatures of either 125 or 170 °C in an ultrahigh-vacuum oven at a pressure lower than 10^{-6} Torr in order to cause the reaction to occur. After annealing, a float transfer method was used to prepare calibration layers for DSIMS in order to allow the deuterium signal from dPS-NH_2 to be related quantitatively to its volume fraction. A 170 nm thick PS film (M_n = 207 kg/mol) was floated on water from a glass slide and transferred on the top of the samples prepared above. Another 100 nm thick dPS film (M_n = 670 kg/mol) floated on water was subsequently transferred on top of the PS calibration layer by the same technique.

Dynamic Secondary Ion Mass Spectrometry (DSIMS). DSIMS is a well-established and widely used depth-profiling technique. Its strength includes relatively good depth resolu-

tion (~8 nm) combined with high sensitivity and the ability to provide the profiles of all elements simultaneously. Particularly, DSIMS is very sensitive to deuterium. Therefore, DSIMS can be a useful tool to detect the diffusion and reaction of deuterium-labeled end-functionalized polymers. Our DSIMS experiments were performed using a Physical Electronics 6650 instrument. Negative ions are detected as polymer is sputtered by an incident beam of 3 keV O_2^+ ions. Our primary aim is to measure the interfacial excess of deuterium-labeled end-grafted PS at the PS/P2VP interface.

Scanning Force Microscopy (SFM). SFM was used to investigate the 2-dimensional interfacial topology. After investigating the depth profile by DSIMS, unreacted dPS-NH_2 and PS homopolymers were removed by washing with a selective solvent, cyclohexane, in an ultrasonic bath at room temperature for 10 min. The sample was then dried in air. A Dimension 3000 SFM from Digital Instruments was used in a tapping mode for all the SFM measurements.

Cross-Sectional Transmission Electron Microscopy (TEM). Cross-sectional TEM samples were prepared on an epoxy substrate. To avoid the dewetting of the PVP film, a 250 nm thick SiO_2 layer was deposited on the epoxy substrate by e-beam thermal evaporation. The PS/P2VP bilayer samples were prepared on the SiO_2-coated epoxy substrate using the same procedure as described above. After annealing in the high vacuum oven, the samples were embedded in epoxy for the microtoming. The samples were microtomed at room temperature into 50 nm thick films using a diamond knife with a Leica Ultracut microtome and then transferred onto lacey carbon-coated grids. The TEM specimen was stained with iodine vapor for 7−10 h. Since the PVP phase was preferentially stained by the iodine vapor, it appears darker than the PS phase in bright field TEM. The interfacial morphology was investigated using a JEOL 2000FX TEM at an accelerating voltage of 200 keV.

Results

The excess amount of dPS-NH_2 at the interface between a PS layer and a P2VP layer during the reaction was monitored by analyzing the deuterium depth profile with DSIMS. This interfacial excess is the evidence of copolymer formation from the reaction of dPS-NH_2 chains with P2VP-ah chains. The volume ratio of end-functionalized polymer to homopolymer in both PS and P2VP layers is fixed at 0.12 initially. The samples were annealed at 170 °C, and the annealing time was varied from 0 to 30 h.

A typical DSIMS depth profile is shown in Figure 2. The interfacial excess z^* of dPS-NH_2 was determined by

$$z^* = \int^{\text{interface}} (\phi(z) - \phi_\infty)\, dz \qquad (1)$$

where $\phi(z)$ is the volume fraction of dPS-NH_2 at a depth z after annealing and ϕ_∞ is the volume fraction of dPS-NH_2 in the bulk of the PS film away from the interface. This excess amount is normalized by the radius of gyration of dPS-NH_2 ($R_{g,PS}$). Figure 3 represents the normalized interfacial excess of dPS-NH_2 (ξ) obtained from a typical DSIMS data series for our system. Up to an annealing time of 10 h, there is a relatively rapid increase in ξ.

As mentioned before, we believe that this interfacial excess comes from diblock copolymer formation by the reaction of dPS-NH_2 chains with P2VP-ah chains. To confirm this hypothesis, control experiments were performed. Identical samples were prepared, except that P2VP-ah was not included in a P2VP layer. Under same annealing conditions, no interfacial excess of copolymer

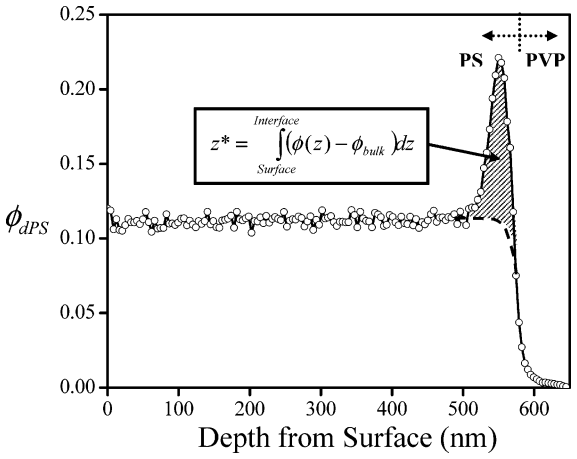

Figure 2. Volume fraction vs depth profile from DSIMS of dPS-NH_2 in a blend of dPS-NH_2 and PS at an interface with a blend of P2VP-ah and P2VP. A line with symbols represents the dPS profile observed by DSIMS after 15 h annealing at 170 °C, and a dotted line represents the unannealed dPS profile which has the same volume fraction of dPS-NH_2 in PS far from the interface. The interfacial integral excess z^* is represented by the shaded area.

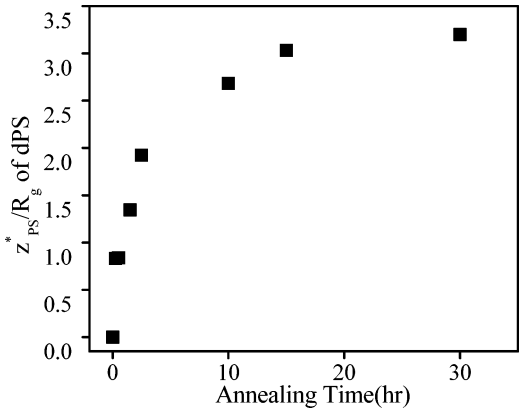

Figure 3. Normalized interfacial excess (ξ) as a function of annealing time at 170 °C for an initial volume fraction ϕ_0 = 0.12.

formation was detected by DSIMS, and no interfacial roughening was found by SFM and cross-sectional TEM.

Direct evidence for the interfacial roughening is provided by SFM images of the annealed samples after washing off the unreacted chains of dPS-NH_2 and the PS homopolymer by using a selective solvent. The interfacial topography was measured for the 4K dPS-NH_2−4K P2VP-ah system with different annealing times. The initial dPS-NH_2 volume fraction (ϕ_0) for the samples shown in Figure 4 was fixed at 0.12. In all experiments, the initial volume fraction of P2VP-ah in a P2VP layer was controlled to be same as that of dPS-NH_2 in a PS layer. Annealing times between 0 and 5 h were explored. While the interface is relatively smooth for the samples whose value of ξ is less than 0.83 as shown in Figure 4a,b, the interface suddenly becomes strongly corrugated for the samples whose value of ξ is 1.35 or larger as shown in Figure 4c,d. Therefore, we can conclude from SFM data that the onset of the interfacial instability takes place between ξ values of 0.83 and 1.35.

Cross-sectional TEM images to support the evidence from the previous section are shown in Figure 5. A 250 nm thick SiO_2 layer was coated on an epoxy substrate

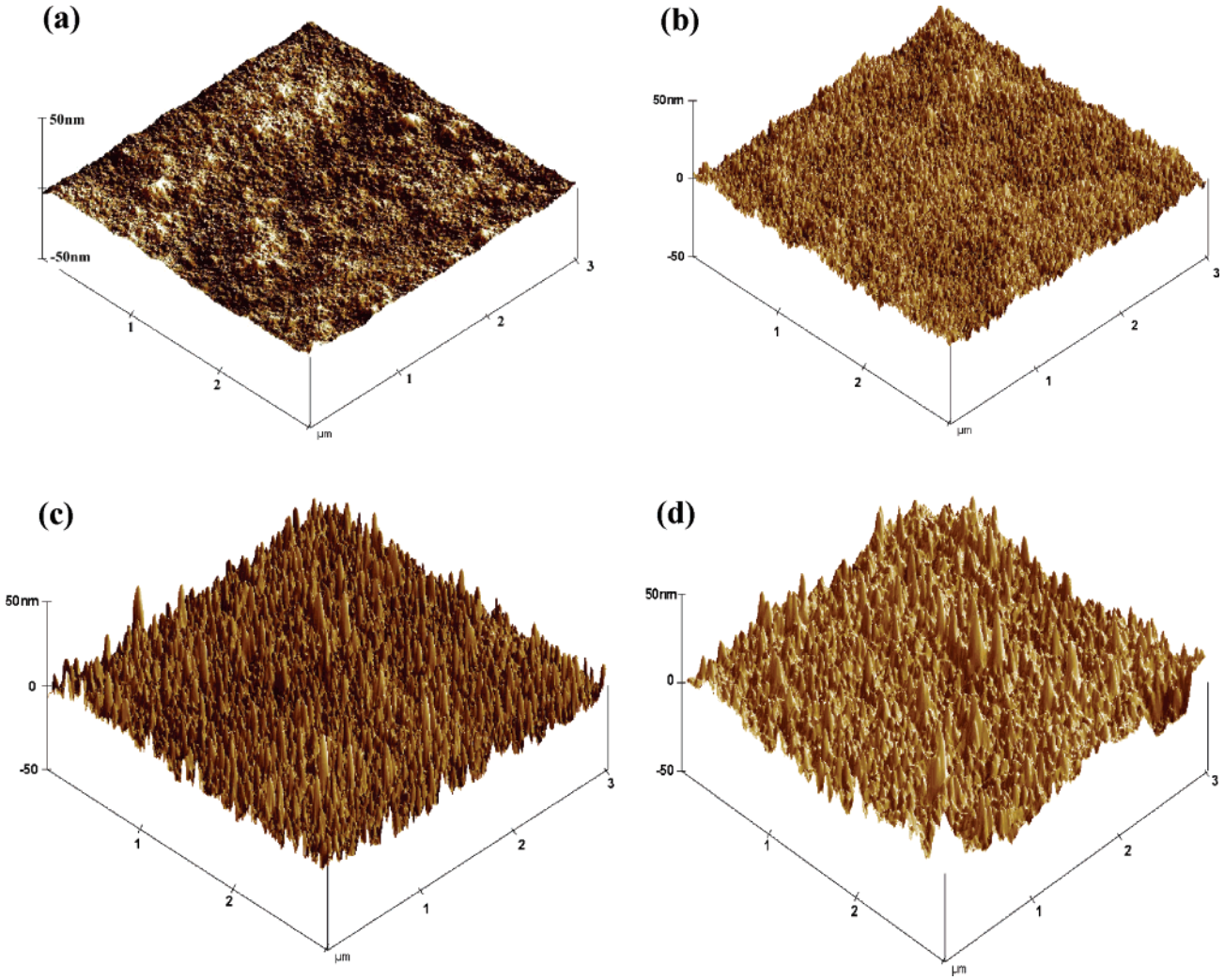

Figure 4. Interfacial roughening probed by SFM as a function of normalized interfacial excess ξ of dPS-NH_2. Samples were annealed at 170 °C. (a) No end-functionalized chains added, $\xi = 0$, roughness (rms) = 1.2 nm; (b) $\xi = 0.83$, rms = 2.2 nm; (c) $\xi = 1.35$, rms = 4.5 nm; (d) $\xi = 1.92$, rms = 5.1 nm.

to provide the identical conditions as the previous samples used in DSIMS and SFM analysis. An initial volume fraction, $\phi_0 = 0.20$, of the end-functionalized polymers was used for the samples in Figure 5. The annealing temperature was decreased from 170 to 125 °C, since the interfacial stress resulting from the large difference in thermal expansion coefficients between the epoxy substrate and the insulating SiO_2 layer cracks the epoxy/SiO_2 interface upon annealing at the temperature of 170 °C. Note that according to SCMFT the dependence of the theoretical critical value of ξ for onset of interfacial roughening on temperature is small in the range between 100 and 200 °C. For example, the predicted critical value of ξ for vanishing of interfacial tension is 1.15 at 170 °C and 1.22 at 125 °C. Therefore, we believe the onset for interfacial roughening in TEM images obtained from the samples annealed at 125 °C is very close to the onset at 170 °C in terms of ξ. Since P2VP is stained by iodine vapor, the darker region of TEM micrographs corresponds to the mixture of P2VP and P2VP-ah, and the brighter region corresponds to the mixture of PS and dPS-NH_2. TEM is a better technique than SFM to investigate the droplets of the polymer microemulsion and micelles that might diffuse from the interface to the surface as well as the interfacial topology, since the SFM images provide only the topology of the interface itself, and this even can sometimes be misleading due to the finite size of a SFM tip. However, the TEM images only show the rough interface in projection through the 50 nm thickness of our microtomed slices. As a result, once the interface becomes rough on a 5 nm scale, it begins to appear blurred in the TEM image. While the interface between PS and P2VP is flat as shown when $\xi = 0.46$ and 0.87 in Figure 5a,b, the interface is not sharp when ξ=1.37 in Figure 5c. We believe that these blurry interfaces were caused mainly by the interfacial roughening by the reaction of end-functionalized polymers. The blurry interfacial region indicates the increase of interfacial width, which was also observed in the DSIMS data. In Figure 5c−e, significant interfacial roughening was observed all over the interface. Diblock copolymer droplets were also found near the PS/P2VP interface. Since symmetric diblock copolymers are formed at the interface, diblock copolymer droplets are found in both layers. However, since the molecular weight of the P2VP matrix (152K) is lower than that of PS (207K), most droplets migrated into the P2VP layer, as shown in Figure 5, parts c, d, and e, where ξ is 1.37, 2.36, and 3.25, respectively. The exact nature of the emulsified droplets remains unclear. However, we can conclude that polymeric droplets shown in Figure 5c−e are formed at the interface and stabilized by diblock copolymer at the interface between the droplets and

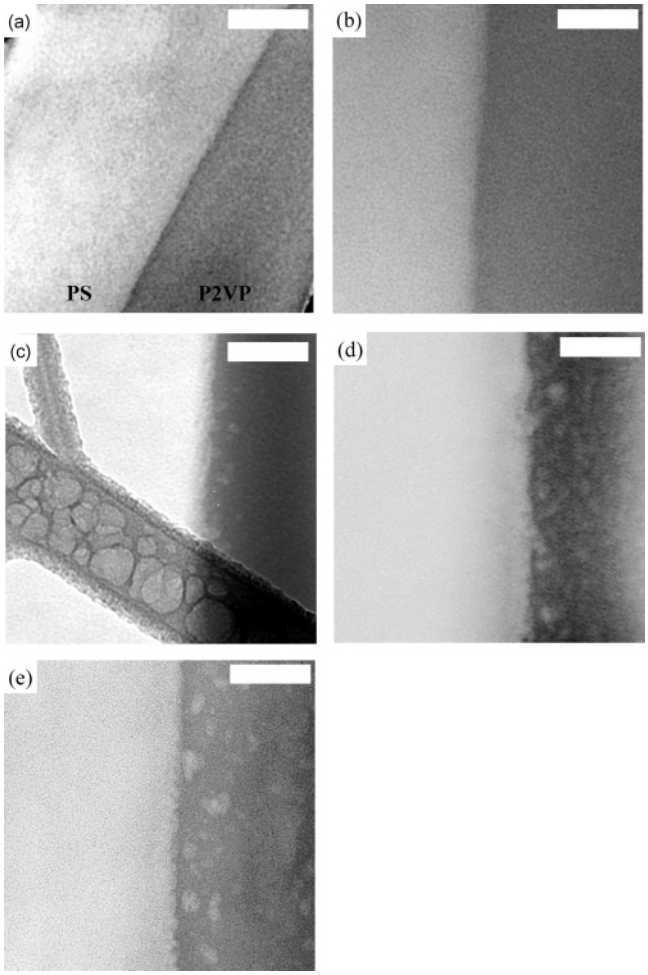

Figure 5. Cross-sectional TEM micrographs of an interface between PS and P2VP after annealing at 125 °C as a function of ξ for an initial volume fraction, $\phi_0 = 0.20$. The darker region corresponds to P2VP by iodine staining. SCMFT estimates that γ approaches zero causing the onset of an interfacial instability as $\xi = 1.22$ at 125 °C. (a) $\xi = 0.46$, (b) $\xi = 0.89$, (c) $\xi = 1.37$, (d) $\xi = 2.36$, and (e) $\xi = 3.25$. Scale bar is 100 nm. The diagonal feature across (c) is a part of the lacy carbon support grid.

homopolymer matrix. This was confirmed by the fact that the movement of block copolymer droplets was consistent with the change of deuterium signal from dPS in diblock copolymers in DSIMS experiments, as shown in Figure 6. The depth profiles of deuterium concentration that comes from dPS-NH_2 for three different values of ξ are shown as a function of depth from the PS top surface. At $\xi = 1.37$, we start to observe a finite but very small of deuterium signal on the right side (the P2VP side) of the interfacial peak. In the TEM image we can observe a small amount of droplets close to the interface. As ξ increases from 1.37 to 3.25, more deuterium is observed in the P2VP layer, indicating that more diblock copolymer coated droplets diffuse into the P2VP layer. Since we observe no droplets in Figure 5b and very few deuterium-labeled chains on the P2VP side of the interface in the corresponding depth profile, we conclude that the diffusion of dPS−PVP diblock copolymer droplets into the P2VP layer only becomes significant after the interface becomes highly corrugated, as shown in TEM images. As shown in Figure 5c−e, the wavelength of the roughened interface is comparable to the diameter of block copolymer droplets. This fact suggests that block copolymer droplets are pinched off

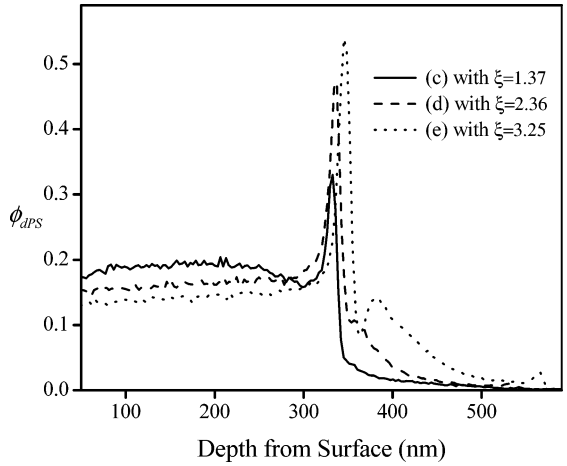

Figure 6. Volume fraction of dPS-NH_2 as a function of depth from the PS top surface obtained by DSIMS. Three different lines represent DSIMS profiles of the samples whose cross-sectional TEM images are shown in Figure 5c−e.

from the interface as the interface becomes rougher and rougher.

Discussion

One of the most important objectives in the current paper is to compare the estimates of the interfacial tension from SCMFT and the Gibbs adsorption equation with the interface morphology obtained from SFM and TEM at a given value of ξ. The easiest way to check this agreement is to investigate the onset of interfacial roughening by SFM and TEM since the onset of interfacial roughening will bring a change in interfacial morphology. First, the interfacial excess value for different annealing times has been calculated from the DSIMS data. Then, using SCMFT, the interfacial tension of our system has been calculated as a function of ξ. Using this approach, the value of ξ for zero interfacial tension can be calculated. These calculated values can be compared with the experimental data for the interfacial roughening obtained from SFM after washing off the top layer using a selective solvent. In the discussion, we will describe how we apply SCMFT and the Gibbs adsorption equation to our system.

Calculation of Interfacial Tension Using SCMFT. One approach to computing the interfacial tension is to use the SCMFT results of Shull[22] for the chemical potential of end-functionalized chains forming a brush at an interface. Since diblock copolymers which contribute to the reduction of interfacial tension at the interface are formed from both the end-functionalized polymers, we can assume that the areal densities of the two end-functionalized polymers are equal

$$\Sigma_{PS} = \frac{z^*_{PS}}{N_{PS}V_{PS}} = \frac{z^*_{PVP}}{N_{PVP}V_{PVP}} = \Sigma_{PVP} \qquad (2)$$

where Σ_{PS} and Σ_{PVP} are the areal densities of dPS-NH_2 and P2VP-ah, respectively, N_{PS} and N_{PVP} are the degrees of polymerization of end-functionalized PS and PVP, respectively, and V_{PS} and V_{PVP} are the volumes of dPS-NH_2 and P2VP-ah, respectively.

From the Gibbs adsorption equation

$$d\gamma = -\sum \varsigma_c \, d\overline{\mu_c} = -\sum \frac{z^*_c}{V_c} d\overline{\mu_c} \qquad (3)$$

where ς_c is the interfacial excess of diblock copolymers formed at the interface in molecules/area, V_c is the volume of diblock copolymers, and $\overline{\mu_c}$ is the chemical potential arising from the entropy loss due to the stretching of diblock copolymers.

Integration of eq 3 gives the interfacial tension as

$$\gamma = \gamma_0 - \int_{-\infty}^{\overline{\mu_c}} \frac{z^*_c(\overline{\mu_c}/k_BT)}{V_c} \, d\overline{\mu_c} = \gamma_0 - \frac{\rho_c R_{g,c}}{N_c} k_BT \int_{-\infty}^{\overline{\mu_c}/k_BT} \frac{z^*_c(\overline{\mu_c}/k_BT)}{R_{g,c}} \, d\left(\frac{\overline{\mu_c}}{k_BT}\right) \quad (4)$$

where γ_0 is the initial interfacial tension without any reaction of end-functionalized polymers, ρ_c is the segmental density of diblock copolymers, and k_B is Boltzmann's constant. γ_0 can be calculated as the following[33,34]

$$\gamma_0 = k_BT\rho_c a\left(\frac{\chi}{6}\right)^{0.5}\left[1 - 2\ln 2\left(\frac{1}{\chi N_{PS}} + \frac{1}{\chi N_{PVP}}\right) + 0.5921\left(\frac{1}{(\chi N_{PS})^{1.5}} + \frac{1}{(\chi N_{PVP})^{1.5}}\right)\right] \quad (5)$$

where χ is the Flory–Huggins interaction parameter, expressed as $\chi = -0.033 + 63/T$ for PS–P2VP[26] and a is the statistical segment length of PS. The statistical segment length and segmental density for P2VP have not been measured but are assumed to be equal to those for PS due to the similarity in segment structure.

For the dry brush limit, Shull[22] has tabulated the values of $\overline{\mu_c}/k_BT$ as a function of $z^*_c/R_{g,c}$ as well as the values for the integral in eq 4. The interfacial tension of the bare interface, γ_0, is predicted to be 3.28×10^{-3} J/m^2 at 170 °C from eq 5. The values of γ can be calculated from Shull's tabulation. The SCMFT estimate for the critical value of $\overline{z^*_c}/R_{g,c}$ where the interfacial tension approaches zero is 1.64 in this system. Since z^*_c is the sum of z^*_{PS} and z^*_{PVP}, eq 2 can be expressed as the following.

$$\xi = \frac{z^*_{PS}}{R_{g,PS}} = \left(\frac{N_{PS}}{N_c}\right)^{0.5}\frac{z^*_c}{R_{g,c}} \quad (6)$$

where N_c is the degree of polymerization of the PS–P2VP diblock copolymer. The interfacial tension of this system is thus expected to vanish when $\xi = z^*_{PS}/R_{g,PS} = 1.15$. The values of γ calculated from Shull's tabulation and the γ_0 value are plotted as a function of ξ in Figure 7.

To check the validity of this simple approach, we have computed γ by a numerical SCMFT technique[35] for the ternary blend system of the diblock copolymers confined to the interface between two immiscible polymers. First, ξ values for zero interfacial tension are calculated as a function of M_n of dPS-NH_2 using eq 5. In the calculation, M_n of P2VP-ah is set to be equal to that of dPS-NH_2. These ξ values for the zero interfacial tension are shown as the line in Figure 8. These results are compared to those from the numerical SCMFT, which are represented by open circles in Figure 8. The agreement between the SCMFT simulations for the ternary blend system and the predictions using Shull's result for the end-functionalized brushes[22] is reasonable. We add the following cautionary note, however. Since Shull's result was obtained for end-adsorbing brushes, it is in principle possible to apply his tabulation in a different way, i.e., by assuming the block copolymer at the interface is made up of two brushes, a PS brush and a PVP one. If we were to sum the separate chemical potentials of the PS brush and the PVP one using Shull's tabulated result for each brush, we arrive at a result that significantly overestimates the decrease of interfacial tension at a given ξ as compared to both the SCMFT and the method outlined above.

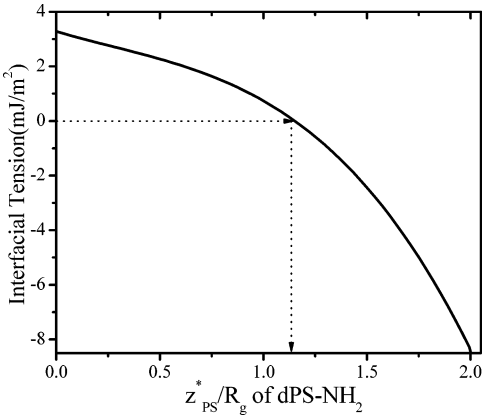

Figure 7. Interfacial tension as a function of ξ at 170 °C calculated by SCMFT. At $\xi = 1.15$, SCMFT estimates that the interfacial tension goes to zero for a short symmetric 4K–4K PS–PVP block copolymer at the PS/PVP interface.

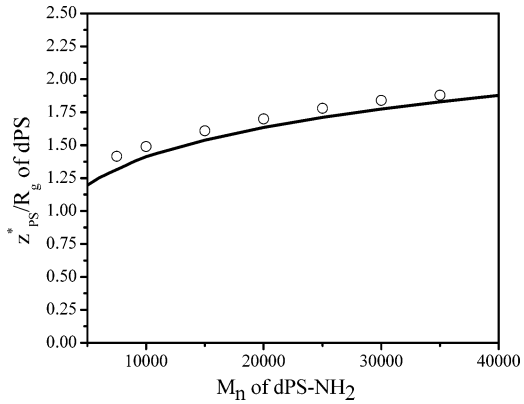

Figure 8. ξ values for zero interfacial tension are shown as a function of M_n of dPS-NH_2. The line represents the result from eq 4, and open circles represent the result from the full SCMFT using a field theoretic simulation method. In both cases, M_n of P2VP-ah is matched with that of dPS-NH_2.

The root-mean-square (rms) roughness of the interfaces determined by SFM for $\phi_0 = 0.12$ is plotted as a function of ξ in Figure 9. While the rms roughness of the interface increases from 1.2 nm to about 2.2 nm as $\xi = z^*/R_g$ increases from 0 to 0.83, it suddenly increases rapidly up to 5 nm at $\xi = 1.35$ as ξ increases further. The increase in interface roughness at low values of ξ where γ is still positive is expected as a result of the increasing amplitude of capillary waves accompanying the decreasing interfacial tension. Note, however, that the major increase in rms roughness occurs for values of ξ around that value ($\xi = 1.15$) where γ of the flat interface is predicted to be zero.

It is important to realize that the values of interfacial tension computed from SCMFT are those predicted for a flat interface. A vanishing of γ implies that the free energy of the system does not increase with increasing interfacial area; thermal fluctuations can then drive interfacial roughening. At the same time once the

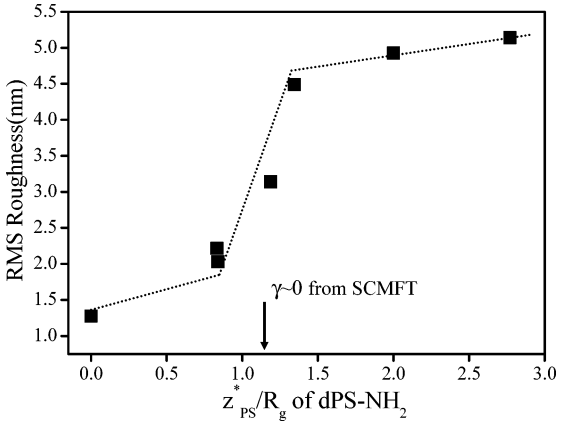

Figure 9. The rms roughness of the interface after removal of the unreacted chains from the P2VP as a function of ξ. The value of the roughness is measured from SFM images of the PS/P2VP interface for $\phi_0 = 0.12$. The onset of zero interfacial tension is predicted by SCMFT to occur at $\xi = 1.15$. The dotted line is a guide to the eye.

interface becomes rough, the SCMFT values for interfacial tension are no longer accurate. The interfacial excess measured by DSIMS is spread over a roughened interface whose area can greatly exceed the nominal area of a flat interface. As the curvature of the interface increases, positive contributions to the free energy result from this curvature[36−38] that is not included in the SCMFT calculation. While it can be anticipated that the local interfacial tension of the curved interface[39] must be at least slightly negative to drive the large scale roughening observed, the exact value achieved will depend in detail on the hydrodynamic flow of the two homopolymer fluids. Under equilibrium conditions the local interfacial tension should be slightly positive.

Our finding that the interface roughens once a critical value of $\xi = z^*/R_g$ is reached, corresponding to that value ξ^* predicted by SCMFT where the interfacial tension vanishes, is broadly consistent with the recent experimental results of Jones et al.,[19] in that in cases where they observed significant roughening by SFM the total amount of block copolymers generated per nominal unit area gives a ξ in excess of ξ^*. They did not attempt to pinpoint the ξ beyond which significant roughening occurred. They argued, however, against the existence of ξ^* claiming that once $\xi > \xi^*$ they would expect complete conversion of end-functionalized chains to block copolymer on the basis of the fact that the interfacial tension goes to zero. Their argument seems to be based on the idea that the end-functionalized polymers become completely miscible in one another once the interfacial tension goes to zero, driven by the increase in ξ, in apparent analogy to what would happen at a critical point in a binary mixture. In contrast to this notion, it seems clear to us that for the ternary system, polymer A, polymer B, and AB diblock copolymers, even if the interfacial tension vanishes as a result of the increase in block copolymer areal density, the interface still exists, and the reaction of chain ends can only occur locally within the interface width.[40]

The exact mechanism of interfacial roughening by reactive polymers is still of considerable controversy. Lyu and co-workers[17] proposed that the interfacial instability is caused by thermal fluctuations of the interface, i.e., capillary waves, that allow the area of the interface to increase, thus allowing more interfacial area for the reaction to occur. If γ remains positive, however, the amplitude of these capillary waves, and thus the extra area generated, remains small. Only if the interfacial tension vanishes can these waves grow substantially in amplitude, and then Lyu et al.'s proposal is identical to ours. In support of this argument, and in complete agreement with our experimental result, the simulations of Yeung and Herrmann[41] showed that the reason for interfacial corrugation is due to the vanishing of interfacial tension. They observed that a significant increase of interface area (or the decrease of areal chain density caused by the increase of interfacial area) and interfacial roughening only occurs after the interfacial tension first vanishes completely. Kim and co-workers[42] also observed that zero interfacial tension was achieved before the interfacial roughening started. They applied the Neumann triangle method to measure the interfacial tension between poly(butylene terephthalate) and PS, and they correlated the measured interfacial tension to the interfacial roughening.

Conclusion

In this paper, the reaction of dPS-NH_2 and PVP-ah at the melt interface between PS and PVP has been investigated experimentally. Diblock copolymers formed at the interface decrease the interfacial tension and ultimately induce interfacial corrugation. The mechanism for interfacial instability was studied by computing the interfacial tension at a given ξ using SCMFT. The amount of diblock copolymer formed was quantified by DSIMS measurements for different reaction times. SCMFT and the Gibbs adsorption equation enable us to calculate the interfacial tension of the system at a given ξ. Therefore, the value of ξ for zero interfacial tension obtained theoretically can be compared to the value of ξ, above which an increase of interfacial roughness is measured experimentally by SFM and TEM. For a short symmetric diblock copolymer, it was found that the interfacial roughening takes place above $\xi = 0.9$, in good agreement with the value where interfacial tension vanishes predicted by SCMFT. Furthermore, it is found that further reaction of end-functionalized polymer induces the formation of block copolymer droplets at the PS/PVP interface. Since the diameter of droplets is about 15 nm, which corresponds to the length scale of interfacial corrugation, the block copolymer droplets appear to be pinched off from the interface.

Acknowledgment. We acknowledge the support of the UCSB Materials Research Lab. (NSF-DMR-MRSEC Grant DMR00-80034). The skillful help of Dr. Tom Mates and Dr. Krystyna Brzezinska of this facility as well as useful discussions with Dr. Ryan Hayward and Dr. Seung-Heon Lee is greatly appreciated.

References and Notes

(1) Creton, C.; Kramer, E. J.; Hadziioannou, G. *Macromolecules* **1991**, *24*, 1848.
(2) Brown, H. R.; Deline, V. R.; Green, P. F. *Macromolecules* **1990**, *23*, 3383.
(3) Brown, H. R.; Char, K.; Deline, V. R.; Green, P. F. *Macromolecules* **1993**, *26*, 4155.
(4) Washiyama, J.; Creton, C.; Kramer, E. J.; Xiao, F.; Hui, C. *Macromolecules* **1993**, *26*, 6011.
(5) Washiyama, J.; Kramer, E. J.; Hui, C. *Macromolecules* **1993**, *26*, 2928.
(6) Char, K.; Brown, H. R.; Deline, V. R. *Macromolecules* **1993**, *26*, 4164.
(7) Welge, I.; Wolf, B. A. *Polymer* **1999**, *42*, 3467.

(8) Leibler, L. *Makromol. Chem., Macromol. Symp.* **1988**, *16*, 1.
(9) Macosko, C. W.; Guégan, P.; Khandpur, A. K.; Nakayama, A.; Marechal, P.; Inoue, T. *Macromolecules* **1996**, *29*, 5590.
(10) Lyu, S.-P.; Jones, T. D.; Bates, F. S.; Macosko, C. W. *Macromolecules* **2002**, *35*, 7845.
(11) Ha, J. W.; Yoon, Y.; Leal, L. G. *Phys. Fluids* **2003**, *15*, 849.
(12) Ramic, A. J.; Stehlin, J. C.; Hudson, S. D.; Jamieson, A. M.; Manas-Zloczower, I. *Macromolecules* **2000**, *33*, 371.
(13) De Gennes, P. G.; Taupin, C. *J. Phys. Chem.* **1982**, *86*, 2294.
(14) Shull, K. R.; Winey, K. I.; Thomas, E. L.; Kramer, E. J. *Macromolecules* **1991**, *24*, 2748.
(15) Jiao, J.; Kramer, E. J.; de Vos, S.; Möller, M.; Koning, C. *Macromolecules* **1999**, *32*, 6261.
(16) Jiao, J.; Kramer, E. J.; de Vos, S.; Möller, M.; Koning, C. *Polymer* **1999**, *40*, 3585.
(17) Lyu, S.-P.; Cernohous, J. J.; Bates, F. S.; Macosko, C. W. *Macromolecules* **1999**, *32*, 106.
(18) Xu, Z.; Jandt, K. D.; Kramer, E. J.; Edgecombe, B. D.; Frechet, J. M. J. *J. Polym. Sci., Part B: Polym. Phys.* **1995**, *33*, 2351.
(19) Jones, T. D.; Schulze, J. S.; Macosko, C. W.; Lodge, T. P. *Macromolecules* **2003**, *36*, 7212.
(20) Yin, Z.; Koulic, C.; Pagnoulle, C.; Jerome, R. *Langmuir* **2003**, *19*, 453.
(21) Kim, H. Y.; Jeong, U.; Kim, J. K. *Macromolecules* **2003**, *36*, 1594.
(22) Shull, K. R. *J. Chem. Phys.* **1991**, *94*, 5723.
(23) Schulze, J. S.; Cernohous, J. J.; Hirao, A.; Lodge, T. P.; Macosko, C. W. *Macromolecules* **2000**, *33*, 1191.
(24) Schulze, J. S.; Moon, B.; Lodge, T. P.; Macosko, C. W. *Macromolecules* **2001**, *34*, 200.
(25) Yokohama, H.; Kramer, E. J. *Macromolecules* **1998**, *31*, 7871.
(26) Dai, K. H.; Kramer, E. J. *Polymer* **1994**, *35*, 160.
(27) Scott, C.; Macosko, C. W. *J. Polym. Sci., Part B: Polym. Phys.* **1994**, *32*, 205.
(28) Padwa, A. R.; Sasaki, Y.; Wolske, K. A.; Macosko, C. W. *J. Polym. Sci., Part A: Polym. Chem.* **1995**, *33*, 2165.
(29) Wang, Z. Y. *Synth. Commun.* **1990**, *20*, 1607.
(30) Dai, K. H.; Kramer, E. J.; Shull, K. R. *Macromolecules* **1992**, *25*, 220.
(31) Dziezok, P.; Sheiko, S. S.; Fischer, K.; Schmidt, M.; Moller, M. *Angew. Chem., Int. Ed. Engl.* **1997**, *36*, 24.
(32) Lim, H.; Lee, Y.; Han, S. H.; Yoo, Y.; Kim, K. J. *Bull. Korean Chem. Soc.* **1999**, *20*, 853.
(33) Helfand, E.; Tagami, Y. *Polym. Lett.* **1971**, *9*, 741.
(34) Semenov, A. N. *J. Phys. II* **1996**, *6*, 1759.
(35) Fredrickson, G. H.; Ganesan, V.; Drolet, F. *Macromolecules* **2002**, *35*, 16.
(36) Goveas, J. L.; Fredrickson, G. H. *J. Rheol.* **1999**, *43*, 1261.
(37) Granek, R.; Ball, R. C.; Cates, M. E. *J. Phys. II* **1993**, *3*, 829.
(38) Müller, M.; Gompper, G. *Phys. Rev. E* **2002**, *66*, 041805.
(39) Wang, Z. G.; Safran, S. A. *J. Chem. Phys.* **1991**, *94*, 679.
(40) Bates, F. S.; Maurer, W. M.; Lipic, P. M.; Hillmyer, M. A.; Almdal, K.; Mortensen, K.; Fredrickson, G. H.; Lodge, T. P. *Phys. Rev. Lett.* **1997**, *79*, 849.
(41) Yeung, C.; Herrmann, K. A. *Macromolecules* **2003**, *36*, 229.
(42) Kim, J. K.; Jeong, W.; Son, J.; Jeon, H. K. *Macromolecules* **2000**, *33*, 9161.

MA047378S